

Article

Developments of Electro-Osmotic Two-Phase Flows of Fourth-Grade Fluid through Convergent and Divergent Channels

Nahid Fatima ¹, Mubbashar Nazeer ², Maha M. A. Lashin ³, M. M. Ghafar ⁴, M. R. Gorji ^{5,*} and M. K. Hameed ⁴

¹ Department of Mathematics and Sciences, Prince Sultan University, Riyadh 11586, Saudi Arabia; nfatima@psu.edu.sa

² Department of Mathematics, Institute of Arts and Sciences, Government College University Faisalabad Chiniot Campus, Chiniot 35400, Pakistan; mubbasharnazeer@gcuf.edu.pk

³ Electrical Engineering Department, College of Engineering, Princess Nourah bint Abdulrahman University, P.O. Box 84428, Riyadh 11671, Saudi Arabia; mmlashin@pnu.edu.sa

⁴ Department of Mathematica, Riphah International University Faisalabad Campus, Faisalabad 38000, Pakistan

⁵ Faculty of Medicine and Health Sciences, Ghent University, 9000 Ghent, Belgium

* Correspondence: mohammad.rahimigorji@ugent.be

Abstract: This paper discusses the development of two different bi-phase flows. Fourth-grade fluid exhibiting the non-Newtonian fluid nature is taken as the base liquid. Two-phase suspension is obtained by using the spherically homogeneous metallic particle. Owing to the intense application of mechanical and chemical multiphase flows through curved and bent configurations effectively transforms the flow dynamics of the fluid. Differential equations for electro-osmotically driven fluid are modeled and solved with the help of the regular perturbation method. The obtained theoretical solution is further compared with the ones obtained by using two different numerical techniques and found to be in full agreement.

Keywords: fourth-grade fluid; homogeneous; configurations; perturbation method suspension

MSC: 35Q35



Citation: Fatima, N.; Nazeer, M.; Lashin, M.M.A.; Ghafar, M.M.; Gorji, M.R.; Hameed, M.K.

Developments of Electro-Osmotic Two-Phase Flows of Fourth-Grade Fluid through Convergent and Divergent Channels. *Mathematics* **2023**, *11*, 1832. <https://doi.org/10.3390/math11081832>

Academic Editors: Ramoshweu Solomon Lebelo, Antonio Lamura and Efstratios Tzirtzilakis

Received: 3 January 2023

Revised: 21 March 2023

Accepted: 10 April 2023

Published: 12 April 2023



Copyright: © 2023 by the authors. Licensee MDPI, Basel, Switzerland. This article is an open access article distributed under the terms and conditions of the Creative Commons Attribution (CC BY) license (<https://creativecommons.org/licenses/by/4.0/>).

1. Introduction

In various applications, the flow of non-Newtonian fluids (such as blood, greases, drilling muds, and suspension, etc.) cannot be expressed by the classical Navier–Stokes theory, and these fluids are categorized as tangent hyperbolic fluids, power-law fluids, generalized Newtonian fluids, Ellis fluids, Williamson fluids, Burgers fluids, Johnson–Segalman fluids, Sisko fluid model, Eyring–Powell fluid, third grade fluid, etc. Due to complex rheological properties and behavior, the fourth-grade fluid [1] is a special type of non-Newtonian fluid that describe the shear thinning and shear thickening phenomena which cannot be expressed by the classical Navier–Stokes equations. The applications of fourth-grade fluids in industry, petroleum and food manufacturing, etc., have significant involvement of diffusion reaction [2] and thermal transports in parallel flows. The constitutive relation [3] of fourth-grade fluid is more complex as compared to second- and third-grade fluids due to more material parameters. So, the study of such highly viscous fluids is hard to model and predict the flow properties, due to scores of parameters. Salawu et al. [4] reported important results on fourth-grade fluid. The investigation is carried out for a parallel flow that obeys the fundamentals of Couette flow mechanism. The numerical results are reached via finite semi-discretization difference method.

Fourth-grade fluid is treated as biological flow in [5] in the curved artery channel by Khan et al. with the help of numerical technique. An approximate study of circular flows with temperature-dependent viscosity of fourth-grade fluid through is the focal

point of different authors in [6,7]. Aziz and Mahomed [8] present a theoretical analysis of fourth-grade fluid over a porous plate.

The flow of bulk fluids through the membrane, porous channel, capillary tube, microchannel, or any other fluid channel under the action of the electric field applied at the end of the conduit is termed electro-osmosis flow. The electroosmotic flow getting the attention of researchers and authors due to its wider applications in medical science, natural chemistry, industrial processes [9], etc. The electro-osmotic flow in non-Newtonian fluids, namely, colloidal suspension, blood, polymeric and protein arrangements, have significant usages. Currently, various studies on the electro-osmotic flow of non-Newtonian fluids have been reported by researchers by considering different constitutive models such as Eyring–Powell fluid [10], Williamson fluid [11], Casson fluid [12], Sutterby fluid [13], generalized Newtonian fluid [14], fractional Maxwell fluid [15], Walters'-B fluid [16], Phan Thien Tanner fluid [17], Power-law fluid [18], Oldroyd-B fluid [19] and third-grade fluid [20], etc.

In addition to the above literature, close analysis of some recent studies on the multiphase flow of fourth-grade fluid under the action of the electric field in two complex configurations, namely, convergent and divergent channels, is a worthwhile investigation. The analysis of this study is a significant contribution to understanding the behavior of the multiphase flow of fourth-grade fluid in terms of physical and mathematical point of view. The modeled highly nonlinear differential equations are dealt with "Perturbation technique" to achieve an approximate solution.

2. Development of a Mathematical Model of Multiphase Flow of Non-Newtonian Fluid with Electro-Osmotic Phenomena

Consider a two-phase flow of fourth-grade fluid through channels as shown in Figures 1 and 2, respectively. The configuration of convergent [21] and divergent [22] channels can be defined as:

Geometry 1:

$$H(x) = \begin{cases} a - b\sqrt{1 - \cos(\frac{\pi x}{\lambda})}; & \text{When } \frac{11\lambda}{7} < x < \frac{33\lambda}{7}, \\ 0.5a; & \text{Othwewise} \end{cases}, \tag{1}$$

Geometry 2:

$$H(x) = \begin{cases} a - b \sin^2(\frac{\pi x}{\lambda}) & \text{When } \frac{11\lambda}{7} < x < \frac{33\lambda}{7}, \\ 0.5a; & \text{Othwewise.} \end{cases} \tag{2}$$

If $\mathbf{V}_{vf} = [u_{vf}(x, y), 0, 0]$ and $\mathbf{V}_{vp} = [u_{vp}(x, y), 0, 0]$ denote the velocity of fluid and particle phase, respectively. The governing equations for this dissemination of fluid and particle phases are:

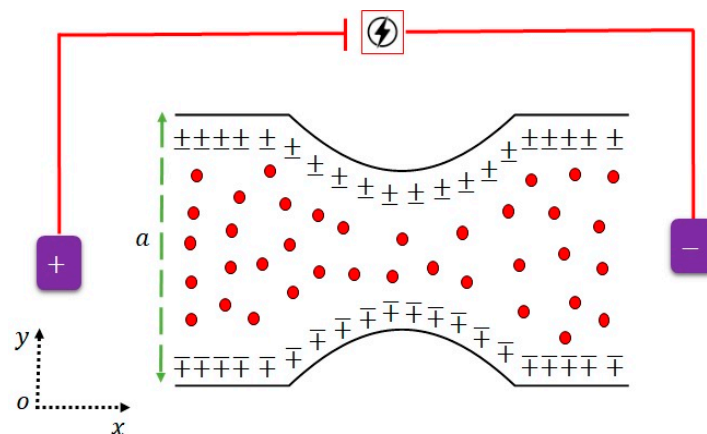


Figure 1. Convergent geometry.

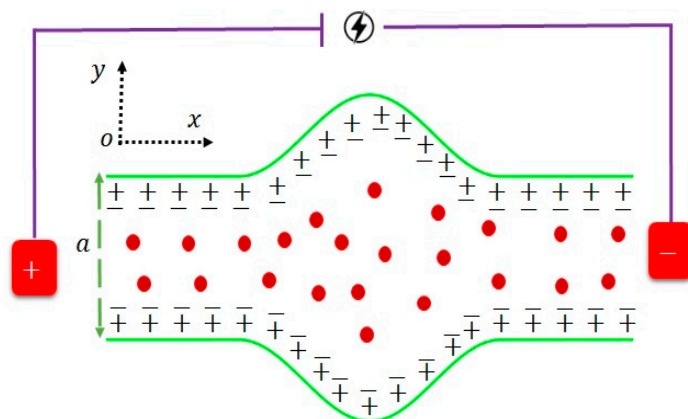


Figure 2. Divergent geometry.

2.1. Flow Equations for Fluid Phase

The equation of continuity which governs the conservation of mass of the flow is

$$\nabla \cdot \mathbf{V}_{vf} = 0, \tag{3}$$

similarly, the conservation of momentum [23,24] for the fluid phase of the considered problem is given as

$$\rho_f(1 - C) \frac{D \mathbf{V}_{vf}}{D t} = -(1 - C) \nabla \cdot p + (1 - C) \nabla \cdot \mathbf{T} - SC(\mathbf{V}_{vp} - \mathbf{V}_{vf}) + \mathbf{J} \times \mathbf{B} + g\rho_f. \tag{4}$$

The mathematical expression of “**T**” is defined as [2]

$$\mathbf{T} = S_1 + S_2 + S_3 + S_4, \tag{5}$$

$$S_1 = \mu \mathbf{A}_1, \tag{6}$$

$$S_2 = \alpha_1 \mathbf{A}_2 + \alpha_1 \mathbf{A}_1^2, \tag{7}$$

$$S_3 = \beta_1 \mathbf{A}_3 + \beta_2 (\mathbf{A}_2 \mathbf{A}_1 + \mathbf{A}_1 \mathbf{A}_2) + \beta_3 (tr \mathbf{A}_1^2) \mathbf{A}_1, \tag{8}$$

$$S_4 = \gamma_1 \mathbf{A}_4 + \gamma_2 (\mathbf{A}_3 \mathbf{A}_1 + \mathbf{A}_1 \mathbf{A}_3) + \gamma_3 \mathbf{A}_2^2 + \gamma_4 (\mathbf{A}_2 \mathbf{A}_1^2 + \mathbf{A}_1^2 \mathbf{A}_2) + \gamma_5 (tr \mathbf{A}_2) \mathbf{A}_2 + \gamma_6 (tr \mathbf{A}_2) \mathbf{A}_1^2 + \gamma_7 (tr \mathbf{A}_3) + \gamma_8 (tr (\mathbf{A}_2 \mathbf{A}_1)) \mathbf{A}_1, \tag{9}$$

$$\mathbf{A}_1 = \mathbf{L} + \mathbf{L}^T, \tag{10}$$

$$\mathbf{A}_n = \frac{d\mathbf{A}_{n-1}}{dt} + \mathbf{A}_{n-1} \mathbf{L} + \mathbf{L}^T \mathbf{A}_{n-1}, \quad n \geq 2, \tag{11}$$

$$\mathbf{L} = \nabla \mathbf{V}_{vf}. \tag{12}$$

In the above one can identify

$$\mathbf{J} = \sigma (\mathbf{E} + \mathbf{V}_{vf} \times \mathbf{B}), \tag{13}$$

The equation of continuity and momentum equations are defined in the following manner

$$\nabla \cdot \mathbf{V}_{vp} = 0, \tag{14}$$

$$\rho_p C \frac{D \mathbf{V}_{vp}}{D t} = -C \nabla \cdot p + -SC(V_{vp} - V_{vf}). \tag{15}$$

It is presumed that the velocity of the bi-phase fluid is zero and the particle concentration remains the same during the study, so the Equations (3), (4), (13) and (15) in the component's forms can be written as

$$\frac{\partial u_{vf}}{\partial y} = 0. \tag{16}$$

The momentum of the fluid phase can be obtained as

$$\rho_f(1 - C) \left(\frac{\partial u_{vf}}{\partial t} + u_{vf} \frac{\partial u_{vf}}{\partial x} + v_{vf} \frac{\partial u_{vf}}{\partial y} \right) = -(1 - C) \frac{\partial p}{\partial x} + (1 - C) \left\{ \mu \frac{\partial^2 u_{vf}}{\partial y^2} + 6\beta \left(\frac{\partial u_{vf}}{\partial y} \right)^2 \left(\frac{\partial^2 u_{vf}}{\partial y^2} \right) \right\} - SC(u_{vp} - u_{vf}) + \left(\frac{\partial^2 \phi}{\partial x^2} + \frac{\partial^2 \phi}{\partial y^2} \right) \vec{E}_x, \text{ where } \beta = \beta_2 + \beta_3. \tag{17}$$

The overhead expression has a lot of significance because if β_3 is zero, the Equation (17) turns into a momentum equation for third-grade fluid and if both are equal to zero, then the resulting equation is also a momentum equation of second-grade Newtonian fluids and if both are not turned into zero the result will be momentum equation of four grade.

$$\rho_f(1 - C) \left(\frac{\partial v_{vf}}{\partial t} + u_{vf} \frac{\partial v_{vf}}{\partial x} + v_{vf} \frac{\partial v_{vf}}{\partial y} \right) = -(1 - C) \frac{\partial p}{\partial y} + (1 - C) \left\{ \alpha \left(\frac{\partial u_{vf}}{\partial y} \right) \left(\frac{\partial^2 u_{vf}}{\partial y^2} \right) + \gamma \left(\frac{\partial u_{vf}}{\partial y} \right)^3 \left(\frac{\partial^2 u_{vf}}{\partial y^2} \right) \right\} - SC(v_{vp} - v_{vf}). \tag{18}$$

where $\alpha = 4\alpha_1 + 2\alpha_2$ and $\gamma = 16(\gamma_3 + \gamma_4 + \gamma_5 + 0.5\gamma_6)$.

2.2. Governing Equations (Particle Phase)

The Equations (14) and (15) can be expressed in the following form as

$$\frac{\partial u_{vp}}{\partial y} = 0. \tag{19}$$

$$\rho_f C \left(\frac{\partial u_{vp}}{\partial t} + u_{vp} \frac{\partial u_{vp}}{\partial x} + v_{vp} \frac{\partial u_{vp}}{\partial y} \right) = -C \frac{\partial p}{\partial x} + SC(u_{vp} - u_{vf}). \tag{20}$$

$$\rho_f C \left(\frac{\partial v_{vp}}{\partial t} + u_{vp} \frac{\partial v_{vp}}{\partial x} + v_{vp} \frac{\partial v_{vp}}{\partial y} \right) = -C \frac{\partial p}{\partial y} + SC(v_{vp} - v_{vf}). \tag{21}$$

For steady flow Equations (17), (18), (20) and (21) gained the shape

$$\left\{ \mu \frac{\partial^2 u_{vf}}{\partial y^2} + 6\beta \left(\frac{\partial u_{vf}}{\partial y} \right)^2 \left(\frac{\partial^2 u_{vf}}{\partial y^2} \right) \right\} - \frac{1}{(1 - C)} \frac{\partial p}{\partial x} + \frac{1}{(1 - C)} \left(\frac{\partial^2 \phi}{\partial x^2} + \frac{\partial^2 \phi}{\partial y^2} \right) \vec{E}_x = 0, \tag{22}$$

$$\frac{\partial p}{\partial y} - \left\{ \alpha \left(\frac{\partial u_{vf}}{\partial y} \right) \left(\frac{\partial^2 u_{vf}}{\partial y^2} \right) + \gamma \left(\frac{\partial u_{vf}}{\partial y} \right)^3 \left(\frac{\partial^2 u_{vf}}{\partial y^2} \right) \right\} = 0, \tag{23}$$

$$C \frac{\partial p}{\partial x} = SC(u_{vp} - u_{vf}). \tag{24}$$

Equation (23), is solved for modified pressure, which gives

$$\frac{\partial p}{\partial y} = 0. \tag{25}$$

The boundary conditions are given as

$$u_{vf}(y) = u_{vf_{at\ wall}}; \text{ When } y = -H(x), \tag{26}$$

$$u_{vf}(y) = u_{vf_{at\ wall}}; \text{ When } y = H(x). \tag{27}$$

3. Dimensionalization of the Problem

To predict the contribution of the most significant variables and parameters, it is mandatory to reduce or accumulate certain quantities which are of the least importance. Therefore, the following dimensionless transformation is of effective use.

$$\left. \begin{aligned} \bar{x} &= \frac{x}{L}, \bar{y} = \frac{y}{L}, \bar{u}_{vf} = \frac{u_{vf}}{u^*}, \bar{u}_{vp} = \frac{u_{vp}}{u^*}, \rho_{rel} = \frac{\rho_f}{\rho_p}, \\ \bar{p} &= \frac{pL}{\mu_s u^*}, \omega = \frac{\beta u^{*2}}{\mu L^2}, M = B_o L \sqrt{\frac{\sigma}{\mu}}. \end{aligned} \right\} \tag{28}$$

The dimensionless form of Equations (20)–(27) is achieved by using the expression defined in Equation (28) in the following form as (bars are omitted)

$$\frac{\partial^2 u_{vf}}{\partial y^2} + 6\omega \left(\frac{\partial u_{vf}}{\partial y} \right)^2 \left(\frac{\partial^2 u_{vf}}{\partial y^2} \right) - \frac{M^2}{(1-C)} u_{vf} - \frac{1}{(1-C)} \frac{\partial p}{\partial x} + \left(\frac{m^2 U_{HS}}{(1-C)} \right) \frac{\cosh(mx)}{\cosh(mh)} = 0, \tag{29}$$

$$u_{vp} = u_{vf} - m_2 \frac{\partial p}{\partial x}, \tag{30}$$

$$u_{vf}(y) = 0; \text{ When } y = -h(x), \tag{31}$$

$$u_{vf}(y) = 0; \text{ When } y = h(x). \tag{32}$$

Similarly, the dimensionless form of the relations described in Equations (1) and (2) are narrated as

$$h(x) = \begin{cases} a - \beta \sqrt{1 - \cos(\pi x)}; & \text{When } 0.5 < x < 4.5, \\ 0.5; & \text{Othwewise.} \end{cases} \tag{33}$$

$$h(x) = \begin{cases} 1 - \beta \sin^2(\pi x) & \text{When } 0.5 < x < 4.5, \\ 0.5; & \text{Othwewise.} \end{cases} \tag{34}$$

We assume that

$$\frac{dp}{dx} = P. \tag{35}$$

Then, Equations (29) and (30) become,

$$\frac{\partial^2 u_{vf}}{\partial y^2} + 6\omega \left(\frac{\partial u_{vf}}{\partial y} \right)^2 \left(\frac{\partial^2 u_{vf}}{\partial y^2} \right) - \frac{M^2}{(1-C)} u_{vf} - \frac{1}{(1-C)} P + \left(\frac{m^2 U_{HS}}{(1-C)} \right) \frac{\cosh(mx)}{\cosh(mh)} = 0, \tag{36}$$

$$u_{vp} = u_{vf} - m_2 P. \tag{37}$$

4. Perturbation Solution

To find the approximate analytical solution to Equation (36) can easily be achieved due to the nonlinear term. Therefore, the most effective and reliable solution with the least margin of error can be obtained if the perturbation technique is applied. For this purpose, we assume that:

$$u_{vf} = u_{vf_0} + \varepsilon u_{vf_1} + \varepsilon^2 u_{vf_2} + o(\varepsilon^3), \tag{38}$$

and more suppose that,

$$\omega = \lambda \epsilon. \tag{39}$$

The above equation ϵ is known as the perturbation parameter. In view of Equations (38) and (39), Equation (36) becomes

$$\begin{aligned} & \frac{\partial^2(u_{vf_0} + \epsilon u_{vf_1} + \epsilon^2 u_{vf_2})}{\partial y^2} + 6\lambda \epsilon \left(\frac{\partial(u_{vf_0} + \epsilon u_{vf_1} + \epsilon^2 u_{vf_2})}{\partial y} \right)^2 \left(\frac{\partial^2(u_{vf_0} + \epsilon u_{vf_1} + \epsilon^2 u_{vf_2})}{\partial y^2} \right) \\ & - \frac{M^2(u_{vf_0} + \epsilon u_{vf_1} + \epsilon^2 u_{vf_2})}{(1-C)} - \frac{1}{(1-C)}P + \left(\frac{m^2 U_{HS}}{(1-C)} \right) \frac{\cosh(mx)}{\cosh(mh)} = 0. \end{aligned} \tag{40}$$

Equating and determining the equation of each order of ϵ^0 , ϵ^1 and ϵ^2 :

$$\epsilon^0 : \frac{\partial^2 u_{vf_0}}{\partial (y)^2} - \frac{M^2}{(1-C)} u_{vf_0} - \frac{1}{(1-C)} P + \left(\frac{m^2 U_{HS}}{(1-C)} \right) \frac{\cosh(mx)}{\cosh(mh)} = 0, \tag{41}$$

$$u_{vf_0}(\pm h(x)) = 0. \tag{42}$$

Similarly,

$$\epsilon^1 : \frac{\partial^2 u_{vf_1}}{\partial y^2} + 6\lambda \left(\frac{\partial u_{vf_0}}{\partial y} \right)^2 \left(\frac{\partial^2 u_{vf_0}}{\partial y^2} \right) - \frac{M^2 u_{vf_1}}{(1-C)} = 0, \tag{43}$$

$$u_{vf_1}(\pm h(x)) = 0, \tag{44}$$

$$\epsilon^2 : \frac{\partial^2 u_{vf_1}}{\partial y^2} + 6\lambda \left(\frac{\partial u_{vf_0}}{\partial y} \right) \left[\left(\frac{\partial u_{vf_0}}{\partial y} \right) \left(\frac{\partial^2 u_{vf_1}}{\partial y^2} \right) + 2 \left(\frac{\partial^2 u_{vf_0}}{\partial y^2} \right) \left(\frac{\partial u_{vf_1}}{\partial y} \right) \right] - \frac{M^2 u_{vf_2}}{(1-C)} = 0, \tag{45}$$

$$u_{vf_2}(\pm h(x)) = 0. \tag{46}$$

The solution to Equation (41) is given below

$$u_{vf_0} = (a_4 \cosh[my] + P(a_5 - a_6 \cosh[ya_1]) + a_7 \cosh[ya_1]). \tag{47}$$

The solution to Equation (43) is given below

$$\left. \begin{aligned} u_{vf_1} = & \left(\frac{a_{34} + a_{35}P + a_{36}P^2 + a_{37}P^3}{a_{36}P^2 + a_{37}P^3} \right) \left(\frac{\cosh[a_1y] - \sinh[a_1y]}{\sinh[a_1y]} \right) + \left(\frac{a_{38} + a_{39}P + a_{40}P^2 + a_{41}P^3}{a_{40}P^2 + a_{41}P^3} \right) \left(\frac{\cosh[a_1y] + \sinh[a_1y]}{\sinh[a_1y]} \right) + \\ & \left(\frac{a_8 y \sinh[ya_1] + a_9 \cosh[ya_1] + a_{10} \cosh[3ya_1] + a_{11} \sinh[2ya_1]}{\sinh[my] + a_{12} \cosh[my](9 - 5 \cosh[2ya_1]) + a_{13} \cosh[my]} \right) \\ & \left(\frac{\sinh[ya_1]^2 + a_{14} \sinh[2my] \sinh[ya_1] + a_{15} \cosh[my]^2 \cosh[ya_1]}{a_{16} y \sinh[ya_1] + a_{17} \cosh[ya_1] + a_{18} \cosh[3ya_1] + a_{19} \sinh[my]} \right) \\ & + P \left(\frac{\sinh[2ya_1] + a_{20} \cosh[my](9 - 5 \cosh[2ya_1]) + a_{21} \cosh[my]}{\sinh[ya_1]^2 + a_{22} \sinh[2my] \sinh[ya_1] + a_{23} \cosh[my]^2 \cosh[ya_1]} \right) \\ & + P^2 \left(\frac{a_{24} y \sinh[ya_1] + a_{25} \cosh[3ya_1] + a_{26} \cosh[ya_1] + a_{27} \sinh[my]}{\sinh[2ya_1] + a_{28} \cosh[my] \cosh[2ya_1] + a_{29} \cosh[my] + a_{30} \cosh[my] \sinh[ya_1]^2} \right) \\ & + P^3 (a_{31} y \sinh[ya_1] + a_{32} \cosh[ya_1] + a_{33} \cosh[3ya_1]). \end{aligned} \right\} \tag{48}$$

The solution of Equation (45) is not presented here due to lengthy expressions that appeared after solving it. The final expression of the velocity can be obtained from Equation (48), i.e.,

$$A_{11} = (a_4 \cosh[my] + P(a_5 - a_6 \cosh[ya_1]) + a_7 \cosh[ya_1]) + \left. \begin{aligned} & \left((a_{34} + a_{35}P + a_{36}P^2 + a_{37}P^3) (\cosh[a_1y] - \sinh[a_1y]) \right. \\ & + (a_{38} + a_{39}P + a_{40}P^2 + a_{41}P^3) (\cosh[a_1y] + \sinh[a_1y]) \\ & + (a_8y \sinh[ya_1] + a_9 \cosh[ya_1] + a_{10} \cosh[3ya_1] + a_{11} \\ & \sinh[2ya_1] \sinh[my] + a_{12} \cosh[my] (9 - 5 \cosh[2ya_1]) \\ & + a_{13} \cosh[my] \sinh[ya_1]^2 + a_{14} \sinh[2my] \sinh[ya_1] + \\ & \left. \left. a_{15} \cosh[my]^2 \cosh[ya_1] \right) \right\} \quad (49) \end{aligned}$$

$$A_{12} = P \left(\begin{aligned} & a_{16}y \sinh[ya_1] + a_{17} \cosh[ya_1] + a_{18} \cosh[3ya_1] + a_{19} \\ & \sinh[my] \sinh[2ya_1] + a_{20} \cosh[my] (9 - 5 \cosh[2ya_1]) \\ & + a_{21} \cosh[my] \sinh[ya_1]^2 + a_{22} \sinh[2my] \sinh[ya_1] + \\ & \left. a_{23} \cosh[my]^2 \cosh[ya_1] \right) + \left. \begin{aligned} & P^2 \left(\begin{aligned} & a_{24}y \sinh[ya_1] + a_{25} \cosh[3ya_1] + a_{26} \cosh[ya_1] + a_{27} \\ & \sinh[my] \sinh[2ya_1] + a_{28} \cosh[my] \cosh[2ya_1] + a_{29} \\ & \cosh[my] + a_{30} \cosh[my] \sinh[ya_1]^2 \end{aligned} \right) + \\ & P^3 (a_{31}y \sinh[ya_1] + a_{32} \cosh[ya_1] + a_{33} \cosh[3ya_1]) \end{aligned} \right\}. \quad (50)$$

$$u_{vf} = A + B + \dots \quad (51)$$

Similarly, we can get the expression for the velocity of the particulate phase u_{vp} .

$$u_p = (a_4 \cosh[my] + P(a_5 - a_6 \cosh[ya_1]) + a_7 \cosh[ya_1]) + \left. \begin{aligned} & \left((a_{34} + a_{35}P + a_{36}P^2 + a_{37}P^3) (\cosh[a_1y] - \sinh[a_1y]) \right. \\ & + (a_{38} + a_{39}P + a_{40}P^2 + a_{41}P^3) (\cosh[a_1y] + \sinh[a_1y]) \\ & + (a_8y \sinh[ya_1] + a_9 \cosh[ya_1] + a_{10} \cosh[3ya_1] + a_{11} \\ & \sinh[2ya_1] \sinh[my] + a_{12} \cosh[my] (9 - 5 \cosh[2ya_1]) \\ & + a_{13} \cosh[my] \sinh[ya_1]^2 + a_{14} \sinh[2my] \sinh[ya_1] + \\ & \left. \left. a_{15} \cosh[my]^2 \cosh[ya_1] \right) \right) + \left. \begin{aligned} & P \left(\begin{aligned} & a_{16}y \sinh[ya_1] + a_{17} \cosh[ya_1] + a_{18} \cosh[3ya_1] + a_{19} \\ & \sinh[my] \sinh[2ya_1] + a_{20} \cosh[my] (9 - 5 \cosh[2ya_1]) \\ & + a_{21} \cosh[my] \sinh[ya_1]^2 + a_{22} \sinh[2my] \sinh[ya_1] + \\ & \left. a_{23} \cosh[my]^2 \cosh[ya_1] \right) \right) + \left. \begin{aligned} & P^2 \left(\begin{aligned} & a_{24}y \sinh[ya_1] + a_{25} \cosh[3ya_1] + a_{26} \cosh[ya_1] + a_{27} \\ & \sinh[my] \sinh[2ya_1] + a_{28} \cosh[my] \cosh[2ya_1] + a_{29} \\ & \cosh[my] + a_{30} \cosh[my] \sinh[ya_1]^2 \end{aligned} \right) + \\ & P^3 (a_{31}y \sinh[ya_1] + a_{32} \cosh[ya_1] + a_{33} \cosh[3ya_1]) - \left(\frac{\mu_s}{a\delta\lambda\sigma} \right) P + \dots \end{aligned} \right\} \quad (52)$$

The volumetric flow rates (fluid and particle phases) can be determined from the following expressions:

$$Q_f = \int_0^{\bar{h}} u_f dy, \quad (53)$$

$$Q_p = \int_0^{\bar{h}} u_p dy. \quad (54)$$

The mathematical expression for the total volumetric flow rate is defined as

$$Q = Q_f + Q_p. \quad (55)$$

The expression for pressure P can be obtained by solving the above Equation (55).

5. Comparative Analysis

The comparison between numerical and perturbation solutions is displayed in Table 1. The perturbation solution is obtained in second order while the numerical solution is obtained through the spectral collocation method. In this method, we discretize the derivatives by using the Jacobi orthogonal polynomials or Chebyshev. The nonlinearity is handled through the Newton–Raphson method and finite difference approximation of the Jacobean (discrete Jacobean). Both solutions are obtained in convergent geometry. For this comparison, we obtained the numerical values of fluid velocity and particle velocity against the variation of the Hartmann number. From Table 1, it can be observed that both solutions are well-matched with each other. To validate the numerical results, we used another scheme, namely, the shooting method, and noted that both numerical results are accurate, as listed in Table 2.

Table 1. Absolute error between perturbation and numerical solutions.

<i>M</i>	Perturbation Solution		Numerical Solution		Absolute Error	
	<i>u_{vf}</i>	<i>u_{vp}</i>	<i>u_{vf}</i>	<i>u_{vp}</i>	<i>u_{vf}</i>	<i>u_{vp}</i>
1.0	1.45064	1.45089	1.45198	1.45001	0.134%	0.088%
2.0	1.35730	1.35744	1.35598	1.35671	0.132%	0.073%
3.0	1.21666	1.21680	1.21549	1.21612	0.117%	0.068%
4.0	1.04626	1.04638	1.04519	1.04590	0.107%	0.048%
5.0	0.86436	0.86446	0.86332	0.86399	0.104%	0.047%

Table 2. Absolute error between shooting method and pseudo-spectral collocation method.

<i>C</i>	Pseudo-Spectral Collocation Method		Shooting Method	
	<i>u_{vf}</i>	<i>u_{vp}</i>	<i>u_{vf}</i>	<i>u_{vp}</i>
0.1	1.41085	1.41110	1.41090	1.41001
0.2	1.33491	1.33506	1.33231	1.33325
0.3	1.23917	1.23932	1.23523	1.23567

6. Results and Discussion

A comprehensive parametric study is carried out in this section. The momentum of the particulate flow is predicted via the change in the numerical values of fourth-grade parameter “ ω ”, electro-osmotic “ m ”, particle concentration “ C ” and volumetric flow rate “ Q ”. Because of the diverse shapes and layout, the velocity acts entirely differently. In Figures 3 and 4, the graphs of the most significant parameter ω , the fourth-grade parameter are drawn against the different values ω in both channels. It is of great interest that the velocity of both phases inclines with the respect to the variation in the dimensionless quantity. However, both geometries affect the flow quite differently. This opposite impression of the geometry of the multiphase flow can easily be apprehended due to Bernoulli’s principle of fluid dynamics.

The variation of the electro-osmotic parameter “ m ” on fluid and particle phases is shown in Figures 5 and 6. It can be viewed from the plotted graphs that the electro-osmotic parameter inversely impacts the velocity profile of the fluid and particle phases, respectively. This inverse relationship introduces a force of hindrance across the flow. Therefore, the momentum of the fluid and particles diminishes gradually. Variation in the concentration of metallic particles is depicted in Figures 7 and 8. Unlike previous graphs, the impact of C is quite different, all depending on the configuration of the geometry through which the bi-phase suspension is transported. The momentum of both phases declines by opting for the convergent channel. On the other hand, there is a tremendous enhancement in the velocity of fluid and particle phases when the channel is considered to be the divergent one.

The volumetric flow rate is also a pivotal parameter of this analytic study. In the most recent decade, when every appliance has reduced in size, the need of the hour is to conduct

such research where micro-size geometries and channels are considered; so, in this regard, the volumetric flow rate is especially important to measure. The volumetric flow rate is also known as the rate of fluid flow or volume velocity. This is the volume of the fluid which is passing through the considered geometry per unit of time. Its units in system international (SI) are cubic meter/second; however, cubic centimeters per minute is also in practice. The volumetric flow rate is mathematically defined as

$$Q = V = \lim_{\Delta t \rightarrow 0} \frac{\Delta V}{\Delta t} = \frac{dV}{dt} \tag{56}$$

and this is the scalar quantity. In Figures 9 and 10, the graphs of the volumetric flow rate are plotted against the different values of the parameters Q for both the phases in convergent and divergent channels. As the values of Q enhanced, the velocity profile of fluidic and particulate phases increased in convergent and divergent channels. The same behavior of the graph has been seen in both phases and the simultaneous effect is observed for diversely shaped convergent and divergent channels. This is because when the volumetric flow rate is increased, the velocity in the geometries experienced pressure and the velocity is enhanced due to extra pressure of the flowing fluid, the fluid entering the channel and gaining high velocity.

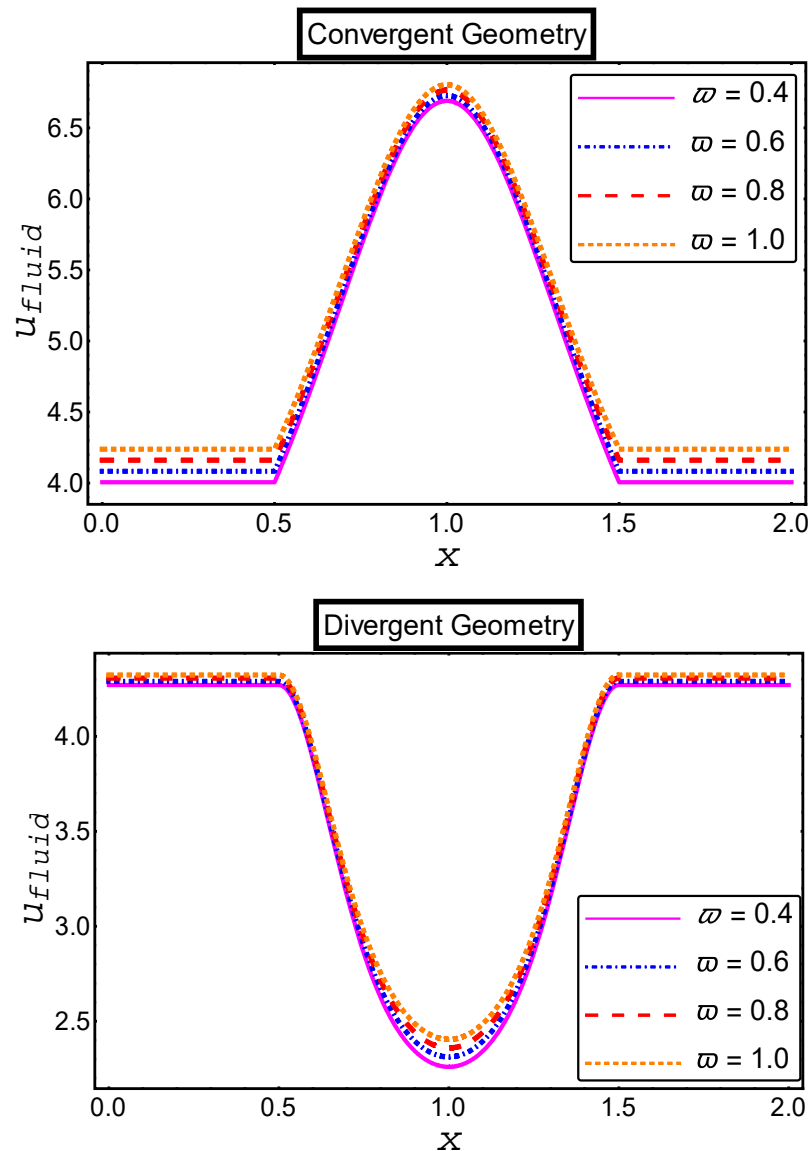


Figure 3. Impact of fourth-grade parameter on fluid velocity.

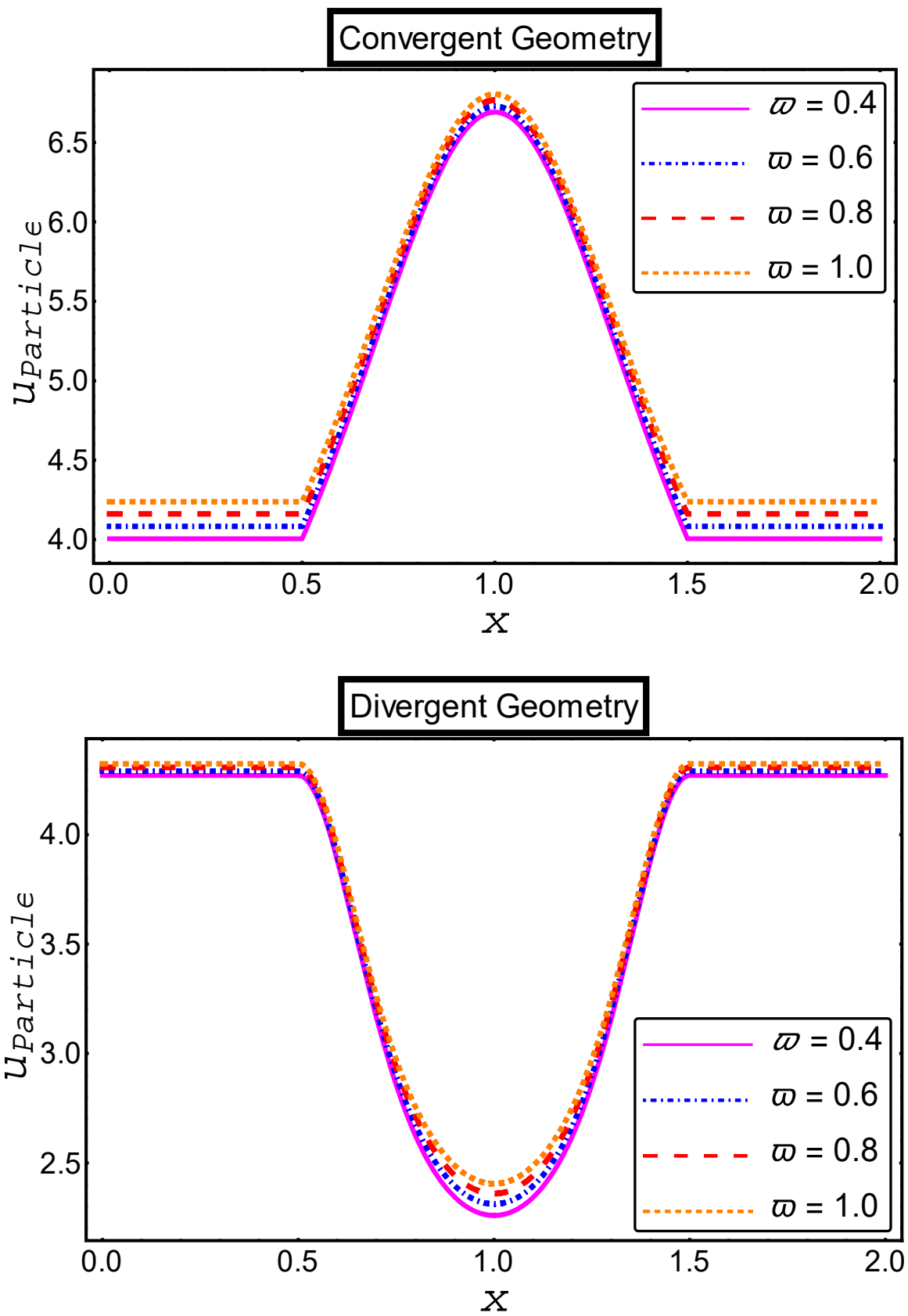


Figure 4. Impact of the four-grade parameter on particle velocity.

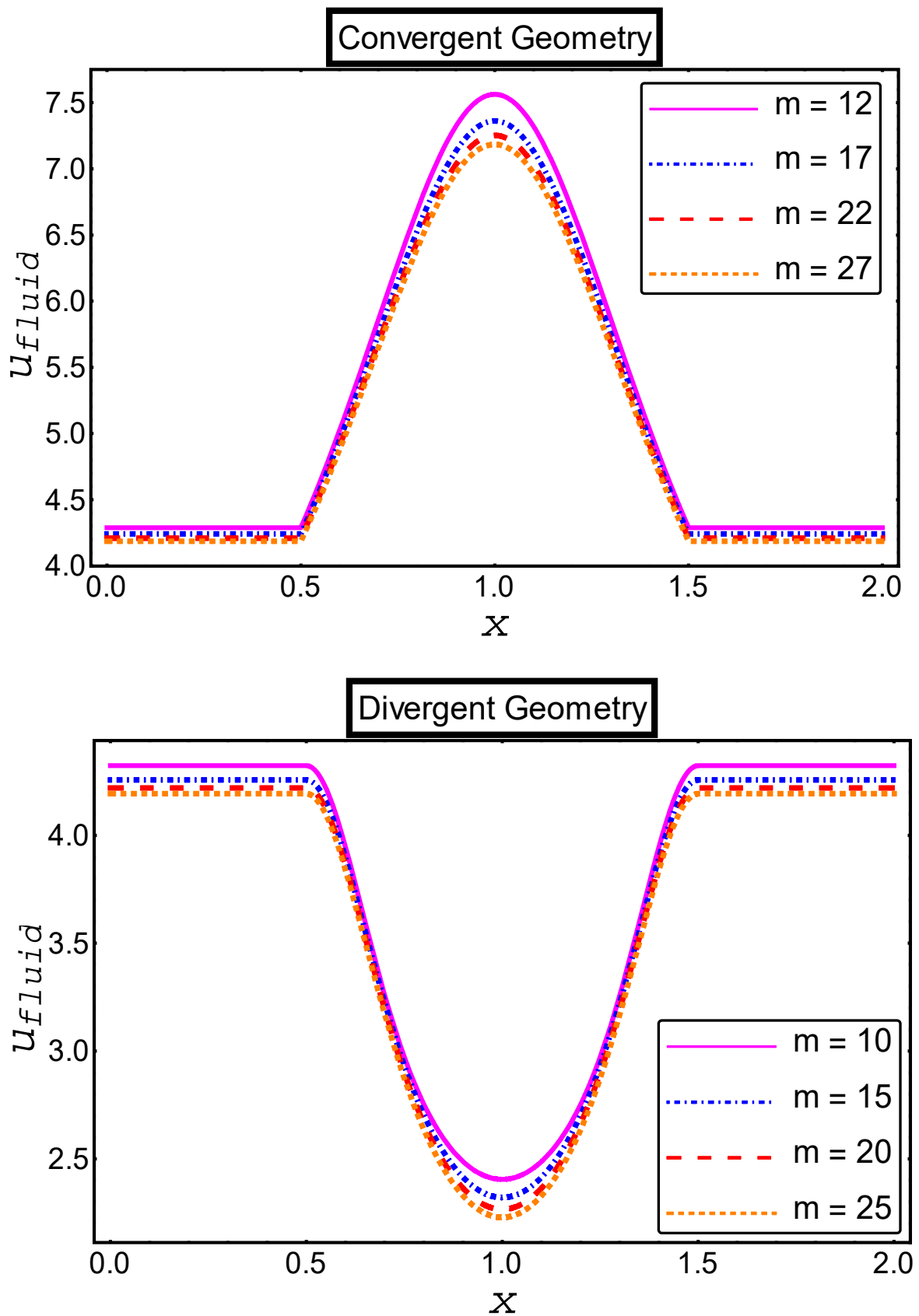


Figure 5. Impact of electro-osmotic parameters on fluid velocity.

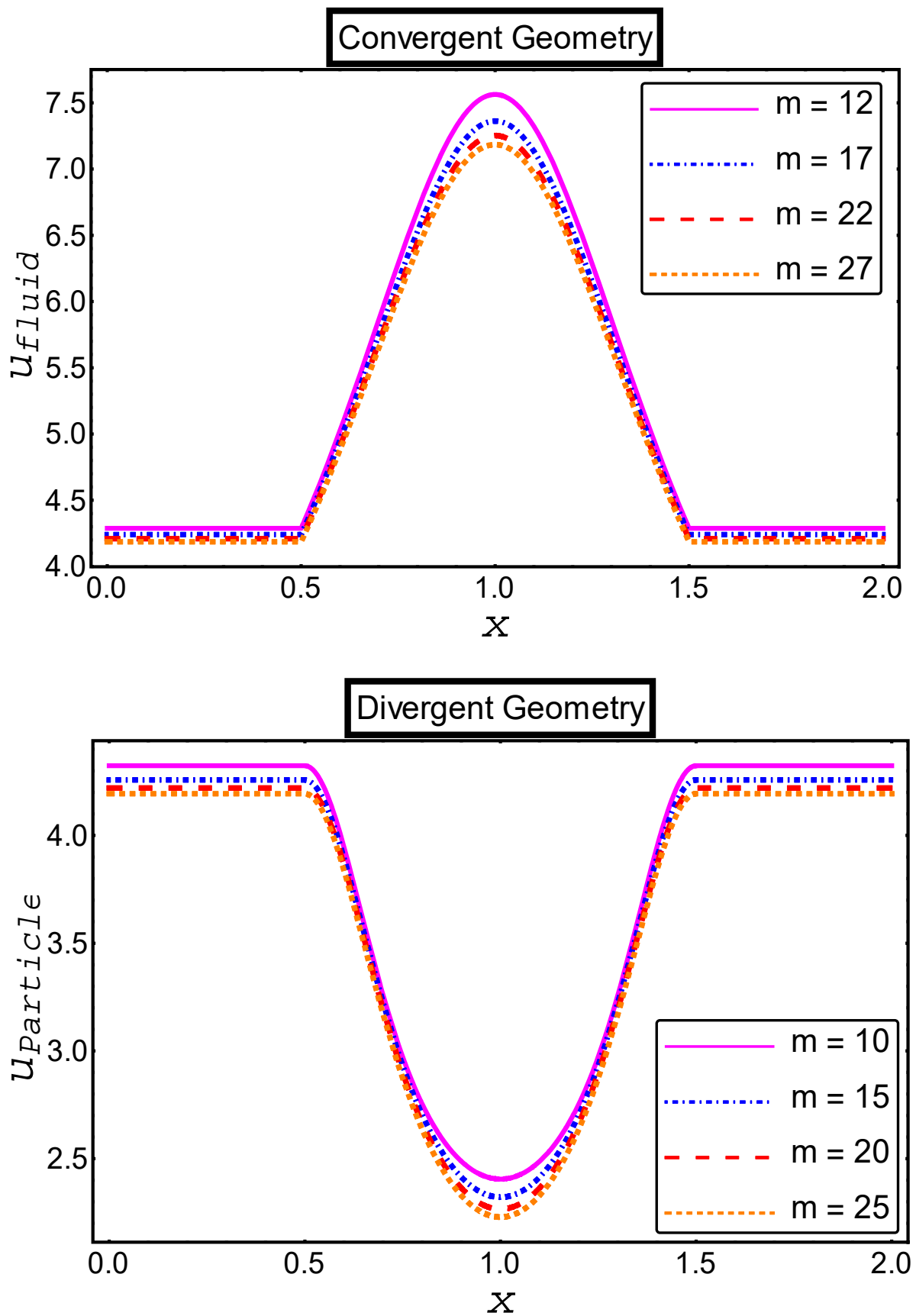


Figure 6. Impact of electro-osmotic parameters on particle velocity.

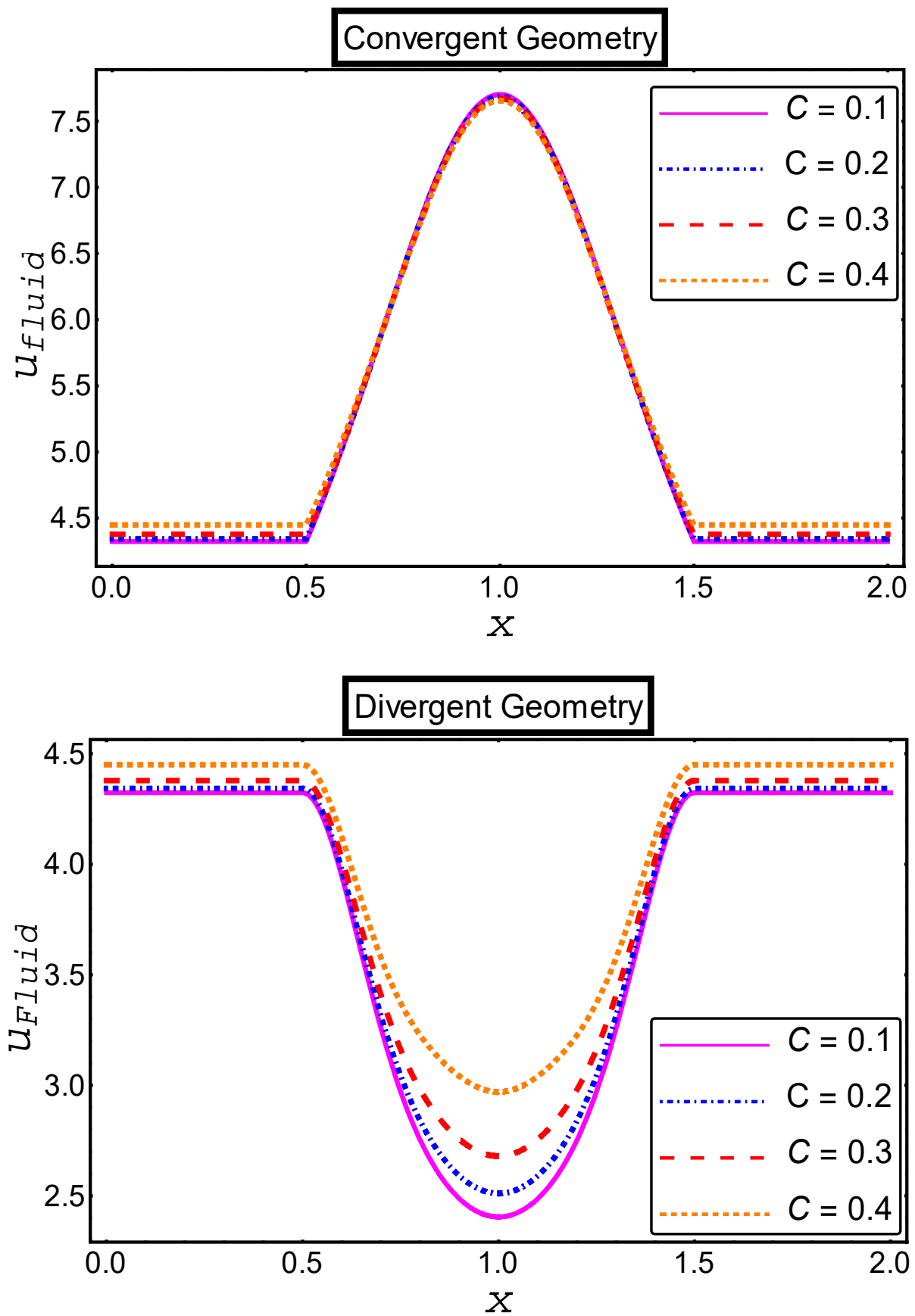


Figure 7. Impact of particle concentration on fluid velocity.

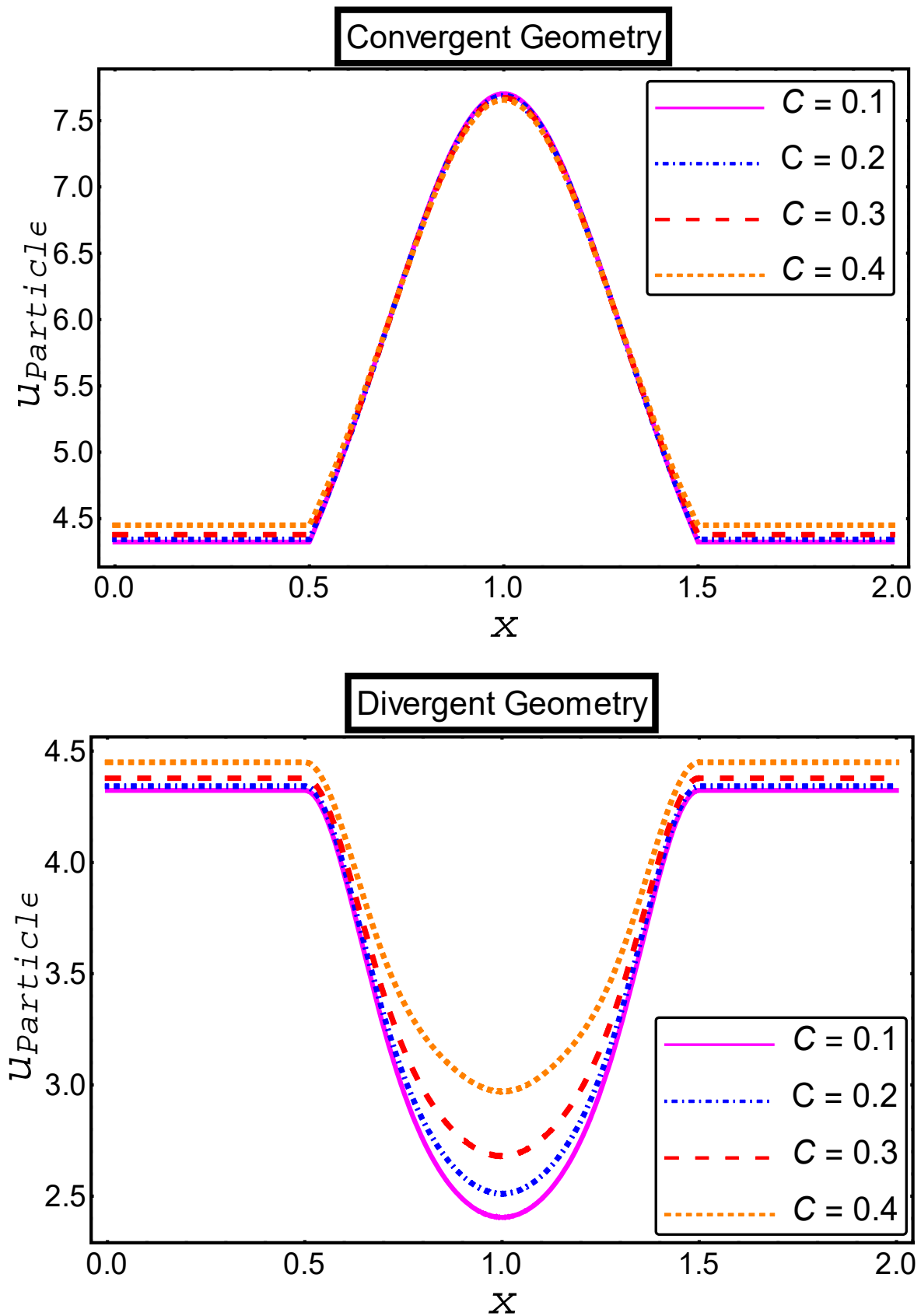


Figure 8. Impact of particle concentration on particle velocity.

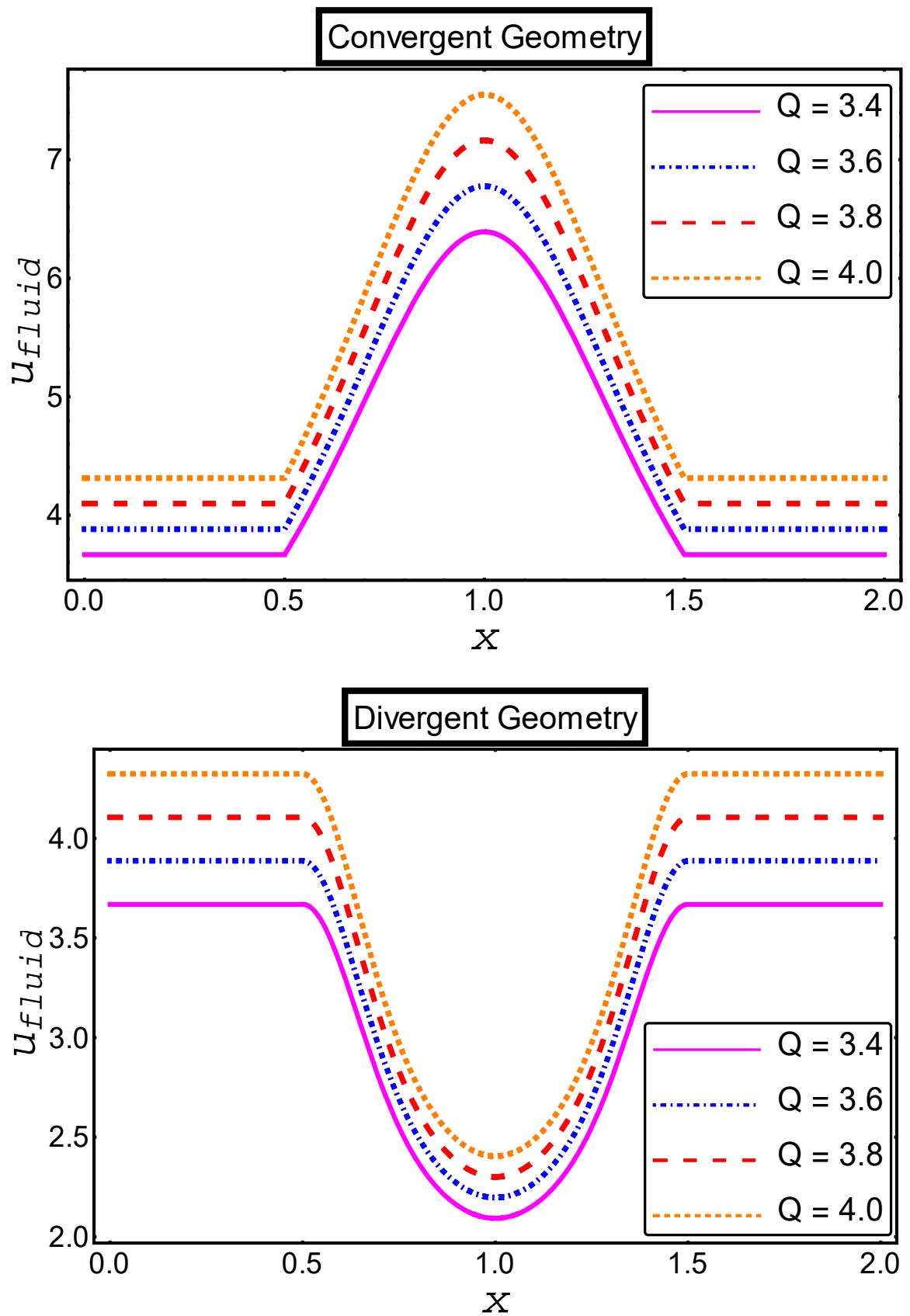


Figure 9. Impact of volumetric flow rate on fluid velocity.

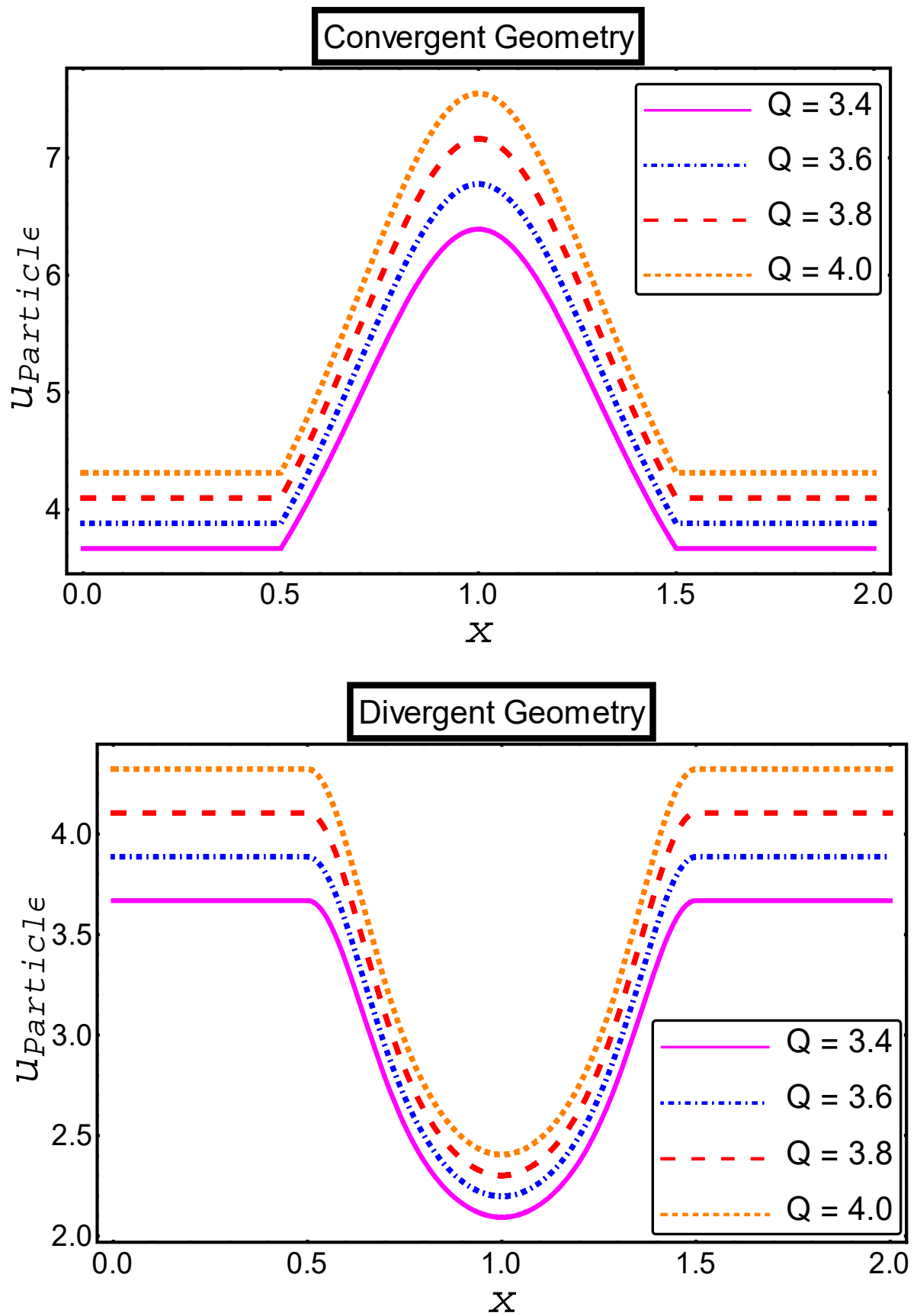


Figure 10. Impact of volumetric flow rate on particle velocity.

7. Concluding Remarks

A closed-form pronouncement for the velocity dispersal of utterly evolve flow of hafnium particles and fourth-grade base fluid adjournment via two different geometries diverse in shape are dispensed. The impact of germane parameters such as fourth-grade parameters, electro-osmotic parameter, the concentration of nanoparticles and volumetric flow rate in a couple of channels such as convergent and divergent flow has been exhibited and inspected graphically. The most noteworthy remarks itemized are:

- ❖ An increase in the behavior of both particle and fluid phase velocities is viewed in convergent and divergent geometries when enhancement is made in the fourth-grade parameter;
- ❖ A remarkable decrease in the velocity profiles of fluid and particle phases in both channels is noted when the value of the electro-osmotic parameter is enhanced;
- ❖ The credible incline is measured in the velocity profile of both phases in the divergent channel when the value of particle concentration is increased, and a very dubious decline has been seen in the velocities of both phases in the convergent channel;
- ❖ When the volumetric flow rate upraised in both channels the velocity profile of fluid and particle phases improved as the volumetric flow rate more in velocities.

Author Contributions: Conceptualization, M.N., M.M.G., M.R.G. and M.K.H.; Methodology, N.F. and M.M.A.L.; Software, M.N. and M.K.H.; Validation, N.F., M.N., M.M.G., M.R.G. and M.K.H.; Formal analysis, M.M.A.L.; Investigation, N.F. and M.R.G.; Data curation, M.M.A.L.; Writing—original draft, M.N., M.M.G. and M.K.H. All authors have read and agreed to the published version of the manuscript.

Funding: This research was funded by [Princess Nourah bint Abdulrahman University, Riyadh, Saudi Arabia] grant number [PNURSP2023R152].

Data Availability Statement: The datasets used and/or analyzed during the current study are available from the corresponding author upon reasonable request.

Acknowledgments: The authors would like to acknowledge Princess Nourah bint Abdulrahman University Researchers Supporting Project number (PNURSP2023R152), Princess Nourah bint Abdulrahman University, Riyadh, Saudi Arabia for their support.

Conflicts of Interest: The authors declare no conflict of interest.

References

1. Islam, S.; Bano, Z.; Siddique, I.; Siddiqui, A. The optimal solution for the flow of a fourth-grade fluid with partial slip. *Comput. Math. Appl.* **2011**, *61*, 1507–1516. [[CrossRef](#)]
2. Hayat, T.; Noreen, S. Peristaltic transport of fourth grade fluid with heat transfer and induced magnetic field. *Comptes Rendus Mécanique* **2010**, *338*, 518–528. [[CrossRef](#)]
3. Sajid, M.; Hayat, T.; Asghar, S. On the analytic solution of the steady flow of a fourth grade fluid. *Phys. Lett. A* **2006**, *355*, 18–26. [[CrossRef](#)]
4. Salawu, S.; Fatunmbi, E.; Ayanshola, A. On the diffusion reaction of fourth-grade hydromagnetic fluid flow and thermal criticality in a plane Couette medium. *Results Eng.* **2020**, *8*, 100169. [[CrossRef](#)]
5. Khan, A.A.; Masood, F.; Ellahi, R.; Bhatti, M. Mass transport on chemicalized fourth-grade fluid propagating peristaltically through a curved channel with magnetic effects. *J. Mol. Liq.* **2018**, *258*, 186–195. [[CrossRef](#)]
6. Sobamowo, M.; Akinshilo, A. Analysis of flow, heat transfer and entropy generation in a pipe conveying fourth grade fluid with temperature dependent viscosities and internal heat generation. *J. Mol. Liq.* **2017**, *241*, 188–198. [[CrossRef](#)]
7. Nadeem, S.; Ali, M. Analytical solutions for pipe flow of a fourth grade fluid with Reynold and Vogel's models of viscosities. *Commun. Nonlinear Sci. Numer. Simul.* **2009**, *14*, 2073–2090. [[CrossRef](#)]
8. Aziz, T.; Mahomed, F. Reductions and solutions for the unsteady flow of a fourth grade fluid on a porous plate. *Appl. Math. Comput.* **2013**, *219*, 9187–9195. [[CrossRef](#)]
9. Yan, S.-R.; Toghraie, D.; Abdulkareem, L.A.; Alizadeh, A.; Barnoon, P.; Afrand, M. The rheological behavior of MWCNTs–ZnO/Water–Ethylene glycol hybrid non-Newtonian nanofluid by using of an experimental investigation. *J. Mater. Res. Technol.* **2020**, *9*, 8401–8406. [[CrossRef](#)]
10. Palencia, J.L.D.; Rahman, S.U.; Redondo, A.N. Regularity and reduction to a Hamilton-Jacobi equation for a MHD Eyring-Powell fluid. *Alex. Eng. J.* **2022**, *61*, 12283–12291. [[CrossRef](#)]

11. Subbarayudu, K.; Suneetha, S.; Ankireddy, B. The assessment of time dependent flow of Williamson fluid with radiative blood flow against a wedge. *Propuls. Power Res.* **2020**, *9*, 87–99. [[CrossRef](#)]
12. Majeed, A.H.; Mahmood, R.; Shahzad, H.; Pasha, A.A.; Raizah, Z.; Hosham, H.A.; Reddy, D.S.K.; Hafeez, M.B. Heat and mass transfer characteristics in MHD Casson fluid flow over a cylinder in a wavy channel: Higher-order FEM computations. *Case Stud. Therm. Eng.* **2023**, *42*, 102730. [[CrossRef](#)]
13. Asfour, H.A.H.; Ibrahim, M.G. Numerical simulations and shear stress behavioral for electro-osmotic blood flow of magneto Sutterby nanofluid with modified Darcy's law. *Therm. Sci. Eng. Prog.* **2023**, *37*, 101599. [[CrossRef](#)]
14. Asghar, Z.; Waqas, M.; Gondal, M.A.; Khan, W.A. Electro-osmotically driven generalized Newtonian blood flow in a divergent micro-channel. *Alex. Eng. J.* **2022**, *61*, 4519–4528. [[CrossRef](#)]
15. Wang, X.; Xu, H.; Qi, H. Numerical analysis for rotating electro-osmotic flow of fractional Maxwell fluids. *Appl. Math. Lett.* **2020**, *103*, 106179. [[CrossRef](#)]
16. Ali, F.; Iftikhar, M.; Khan, I.; Sheikh, N.A.; Aamina; Nisar, K.S. Time fractional analysis of electro-osmotic flow of Walters's-B fluid with time-dependent temperature and concentration. *Alex. Eng. J.* **2019**, *59*, 25–38. [[CrossRef](#)]
17. Trivedi, M.; Maurya, S.; Nirmalkar, N. Numerical simulations for electro-osmotic flow of PTT fluids in diverging microchannel. *Mater. Today Proc.* **2022**, *57*, 1765–1769. [[CrossRef](#)]
18. Miao, H.; Dokhani, V.; Ma, Y.; Zhang, D. Numerical modeling of laminar and turbulent annular flows of power-law fluids in partially blocked geometries. *Results Eng.* **2023**, *17*, 100930. [[CrossRef](#)]
19. Pan, T.-W.; Chiu, S.-H. A DLM/FD method for simulating balls settling in Oldroyd-B viscoelastic fluids. *J. Comput. Phys.* **2023**, *484*, 112071. [[CrossRef](#)]
20. Tahraoui, Y.; Cipriano, F. Optimal control of two dimensional third grade fluids. *J. Math. Anal. Appl.* **2023**, *523*, 127032. [[CrossRef](#)]
21. Mekheimer, K.S.; El Shehawey, E.F.; Elaw, A.M. Peristaltic Motion of a Particle-Fluid Suspension in a Planar Channel. *Int. J. Theor. Phys.* **1998**, *37*, 2895–2920. [[CrossRef](#)]
22. Hussain, F.; Ellahi, R.; Zeeshan, A. Mathematical Models of Electro-Magnetohydrodynamic Multiphase Flows Synthesis with Nano-Sized Hafnium Particles. *Appl. Sci.* **2018**, *8*, 275. [[CrossRef](#)]
23. Ellahi, R.; Zeeshan, A.; Hussain, F.; Abbas, T. Thermally Charged MHD Bi-Phase Flow Coatings with Non-Newtonian Nanofluid and Hafnium Particles along Slippery Walls. *Coatings* **2019**, *9*, 300. [[CrossRef](#)]
24. Ellahi, R.; Zeeshan, A.; Hussain, F.; Abbas, T. Two-Phase Couette Flow of Couple Stress Fluid with Temperature Dependent Viscosity Thermally Affected by Magnetized Moving Surface. *Symmetry* **2019**, *11*, 647. [[CrossRef](#)]

Disclaimer/Publisher's Note: The statements, opinions and data contained in all publications are solely those of the individual author(s) and contributor(s) and not of MDPI and/or the editor(s). MDPI and/or the editor(s) disclaim responsibility for any injury to people or property resulting from any ideas, methods, instructions or products referred to in the content.